Microbiology (2006), **152**, 3575–3583 DOI 10.1099/mic.0.28881-0

Bacterial adhesion to and viability on positively charged polymer surfaces

Akihiko Terada,[1]† Atsushi Yuasa,[1] Takashi Kushimoto,[1] Satoshi Tsuneda,[1] Akio Katakai[2] and Masao Tamada[2]

[1]Department of Chemical Engineering, Waseda University, Ohkubo 3-4-1, Shinjuku-ku, Tokyo 169-8555, Japan

[2]Takasaki Advanced Radiation Research Institute, Japan Atomic Energy Agency, 1233 Watanuki, Takasaki, Gunma 370-1292, Japan

Correspondence
Satoshi Tsuneda
stsuneda@waseda.jp

Received 30 January 2006
Revised 14 August 2006
Accepted 22 August 2006

Secondary and tertiary amino groups were introduced into polymer chains grafted onto a polyethylene flat-sheet membrane to evaluate the effects of surface properties on the adhesion and viability of a strain of the Gram-negative bacterium *Escherichia coli* and a strain of the Gram-positive bacterium *Bacillus subtilis*. The characterization of the surfaces containing amino groups, i.e. ethylamino (EA) and diethylamino (DEA) groups, revealed that the membrane potentials are proportional to amino-group densities and contact angle hysteresis. A high bacterial adhesion rate constant *k* was observed at high membrane potential, which indicates that membrane potential could be used as an indicator for estimating bacterial adhesion to the EA and DEA sheets, especially in *B. subtilis*. The bacterial adhesion rate constant of *E. coli* markedly increased at a membrane potential higher than −7·8 mV, whereas that of *B. subtilis* increased at a membrane potential higher than −8·3 mV, at which the dominant effect on bacterial adhesion is expected to change. The viability experiments revealed that approximately 80 % of *E. coli* cells adhering to the sheets with high membrane potential were inactivated after a contact time of 8 h, whereas 60 % of *B. subtilis* cells were inactivated. Furthermore, *E. coli* viability significantly decreased at a membrane potential higher than −8 mV, whereas *B. subtilis* viability decreased as membrane potential increased, which reflects differences in cell wall structure between *E. coli* and *B. subtilis*.

INTRODUCTION

The vast majority of bacteria adhere to most surfaces and form complex and heterogeneous microbial communities termed biofilms (Bos *et al.*, 1999). Although the formation of biofilms is undesirable in water supply systems and biomaterial systems (Hallam *et al.*, 2001; Hendricks *et al.*, 2000; Kjellerup *et al.*, 2003), the use of biofilms in wastewater treatment systems can be beneficial (Lin *et al.*, 2004; Nicolella *et al.*, 2000). In the former cases, most research is directed to prevention of bacterial adhesion and the subsequent formation of undesirable biofilms. In the latter case, the enhancement of initial adhesion of bacteria to a substrate and the subsequent formation of robust biofilms are important for the rapid startup of biofilm reactors and the effective removal of contaminants by the reactors. Understanding the mechanisms of biofilm formation and development are therefore crucial for inhibiting the formation of undesirable biofilms and promoting the establishment of useful biofilms.

Bacterial adhesion resulting in a stable, mature biofilm generally entails two steps: a reversible step involving physico-chemical forces, and an irreversible step involving physico-chemical and chemical forces such as short-range forces, e.g. hydrophobic/hydrophilic interactions and interactions between strongly localized functional groups on bacterial cells and material surfaces; after the adhesion, the bacteria produce extracellular polymeric substances (EPS) to form the mature biofilm. The significance of the effect of the initial bacterial adhesion on biofilm formation has been questioned because the number of bacterial cells involved in the initial adhesion is much smaller than that in mature biofilms (Fox *et al.*, 1990; Petrozzi *et al.*, 1993); however, some researchers have suggested that there is a link between the initially adhering bacteria and the biofilms which subsequently form (Busscher *et al.*, 1995). In particular, it has been reported that physico-chemical properties, e.g. surface potential,

†Present address: Institute of Environment and Resources, Technical University of Denmark, DK-2800 Lyngby, Denmark.

Abbreviations: DEA, diethylamino; *dg*, degree of grafting; EA, ethylamino; EPS, extracellular polymeric substances; GMA, glycidyl methacrylate; PE, polyethylene; RIGP, radiation-induced graft polymerization.

Five supplementary figures are available with the online version of this paper.

roughness and hydrophobicity, affect the rate of the initial bacterial adhesion and subsequent biofilm formation (Gottenbos *et al.*, 1999, 2000, 2001; Hibiya *et al.*, 2000; Terada *et al.*, 2005). In view of this link, elucidation of details of the mechanism of initial biofilm formation would be useful for understanding techniques to inhibit or promote the formation of biofilms.

Many surface modification techniques, such as surface abrasion (Morgan & Wilson, 2001), chemical coating (Harris & Richards, 2004) and chemical grafting (Gottenbos *et al.*, 1999, 2000, 2001; Hibiya *et al.*, 2000; Lee *et al.*, 1996, 1997, 1998; Park *et al.*, 1998; Pasmore *et al.*, 2001; Roosjen *et al.*, 2003, 2004; Terada *et al.*, 2004, 2005; Wang *et al.*, 2000), have been used to investigate the possibility of inhibiting or promoting bacterial adhesion and biofilm formation. Radiation-induced grafting technology can generate highly reactive radicals and subsequently initiate the polymerization and extension of long graft chains on common polymer materials such as polyethylene (PE). In particular, radiation-induced graft polymerization (RIGP) can control the density and length of graft chains, both of which can be varied by adjusting two set times: the time for which a base material is exposed to an electron beam and the time for which the treated base material is reacted with the vinyl monomer (Kawai *et al.*, 2003). Another important feature of RIGP is that many monomers can be further chemically modified during a functionalization step to improve important properties such as the ability to attract bacterial cells. Such advantages of RIGP allow finer analysis of the relationships between bacterial cells and surfaces. In a previous study, positively or negatively charged groups were added to PE membrane sheets by RIGP of an epoxy-group-containing monomer, glycidyl methacrylate (GMA), and a subsequent epoxy-ring-opening reaction, to determine the effects on bacterial adhesion, and it was found that electrostatic interaction is the most important factor (Terada *et al.*, 2005). However, it is still unclear how positively charged surfaces affect bacterial viability and whether optimal conditions for biofilm inhibition and promotion exist; understanding of these issues would aid in the elucidation of the mechanisms involved in the formation of biofilms, and ultimately lead to strategies for controlling biofilms.

In this study, secondary and tertiary amino groups having positive charges of differing strengths were added to poly-GMA chains. There were two objectives: (1) to examine the effects of the electrostatic properties of a positively charged surface prepared by RIGP on initial bacterial adhesion, and (2) to evaluate the viability of bacteria adhering to surfaces and determine the factors which are important in bacterial viability.

METHODS

Bacterial strains. As representatives of Gram-positive and Gram-negative bacteria, strains of *Bacillus subtilis* (NBRC-3335) and *Escherichia coli* (NBRC-3301) were obtained from the Biological Resource Center of the National Institute of Technology and Evaluation (NBRC) in Japan. Before adhesion tests, these strains were aerobically cultured for 1 day at 30 °C in a liquid medium containing the following: polypeptone, 10·0 g; yeast extract, 5·0 g; sodium chloride, 1·0 g; and distilled water, 1 l. Cells were harvested in their exponential growth phase by centrifugation (8000 ***g***, 10 min) and were resuspended in water. This washing step was repeated three times to eliminate residual substances and EPS. Finally, the washed cells were suspended in 0·02× PBS (pH 7·2). The linear relationship between cell number and OD_{660} was confirmed using YO-PRO-1 (Molecular Probes).

Addition of anion-exchange groups to membrane sheets. Fig. 1 shows the preparation scheme for addition of amino groups to polyethylene (PE). PE-based membrane sheets (PE sheets; Hipore, Asahi Kasei Chemicals, Tokyo, Japan) were used as the trunk polymer for grafting. Each sheet was 10 cm × 7·5 cm, with a porosity of 70 % and a mean pore size of 0·20 μm. Technical-grade GMA was purchased from Tokyo Chemical Industry (formerly Tokyo Kasei Kogyo; Tokyo, Japan) and was used without further purification. Ethylamine and diethylamine were obtained from Kanto Chemical (Tokyo, Japan). The sheets were irradiated with an electron beam from an accelerator (Dynamitron, model IEA 3000-25-2, Radiation Dynamics) operating at a beam energy of 2·0 MeV and a current of 1 mA at ambient temperature in a nitrogen atmosphere. The total irradiation dose was 200 kGy. Then, the irradiated sheets were immersed in a glass ampoule containing GMA (5 %, w/w, in methanol), previously sparged with nitrogen gas, and allowed to react at 40 °C. The radicals generated on the sheets, which react with GMA, were used as starting sites for the polymerization and extension of

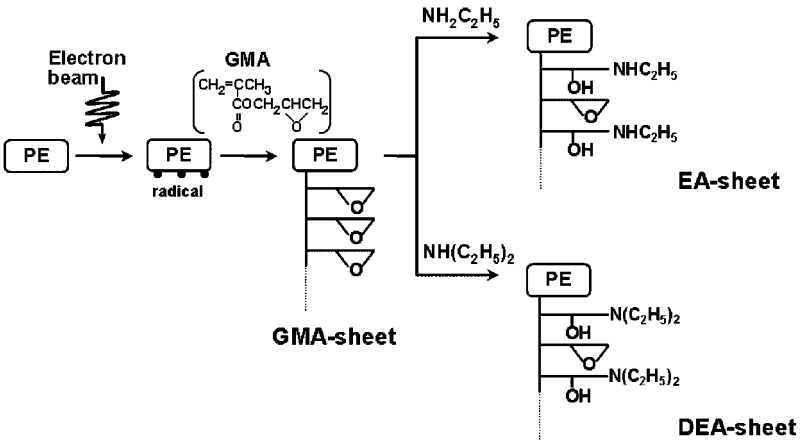

Fig. 1. Preparation scheme for secondary or tertiary amino group-containing polymer chains grafted onto flat-sheet membranes.

long graft chains from the surface of the sheets. The GMA-grafted sheets (GMA sheets) thus obtained were immersed in *N*,*N*′-dimethylformamide and then in methanol to thoroughly remove residual monomers and homopolymers, followed by drying under reduced pressure (Kawai *et al.*, 2000). The amount of GMA grafted onto each stem sheet represented the degree of grafting (*dg*) calculated using the formula

$$dg = 100 \times \left(\frac{W_1 - W_0}{W_0} \right) \quad (1)$$

where W_0 and W_1 are the weights of the stem sheet and the GMA sheet, respectively. Grafted sheets with *dg* values of approximately 100 % and 200 % were prepared by setting the grafting time at 30 and 60 min, respectively. The GMA sheets were then immersed in 50 % (v/v) ethylamine- or diethylamine-containing solution (solvent: water) at 30 °C. The reaction of the GMA sheets with EA and DEA converts the epoxy groups of the GMA into the respective amino groups. The amino group density and molar conversion percentage were calculated using

$$\text{Amino group density} = 1000 \times \frac{\frac{W_2 - W_1}{M_r}}{W_2} \quad (2)$$

$$\text{Molar conversion percentage of amino groups} = 100 \times \frac{\frac{W_2 - W_1}{M_r}}{\frac{W_1 - W_0}{142}} \quad (3)$$

where W_2 and M_r are the weight of the amino-group-containing sheet and the relative molecular mass, respectively. Hereafter, the resultant GMA-, EA- and DEA-containing sheets are respectively referred to as GMA, EA and DEA (*X*) sheets; *X* in parentheses designates the molar conversion percentage of each amino group.

Characterization of membrane sheets prepared by RIGP. The densities of the EA and DEA groups were determined from the measurements of the total ion-exchange capacity by titration. The EA and DEA sheets were immersed in 2 M NaOH to recover anion-exchange capacity. Then 0·2 M HCl was used for ion exchange. Titration was performed using 0·1 M NaOH. A solution of methyl red and methylene blue (Kanto Chemical) was used as an indicator. Membrane potential was measured by the method of Tsuru *et al.* (1990). A U-bend glass cell was divided into two compartments by pinching one membrane sheet at the bottom of the cell. After rinsing in distilled water, the membrane sheets were used for the measurements. Distilled water and 0·02 M PBS (pH 7·2) were supplied to one side and the other side of the cell, respectively. Temperature was maintained at 25 °C. Membrane potential was measured using two reference electrodes (RE-1C, BAS, Tokyo, Japan), which were Ag/AgCl electrodes, both connected to an electrometer (R8240, Advantest, Tokyo, Japan) in saturated KCl solution. The measurement was conducted in triplicate under the same conditions. The surface dynamics of the prepared surfaces were measured using the dynamic Wilhelmy plate technique. Surface tension–immersion depth hysteresis curves in ultrapure water were obtained using a dynamic contact angle measurement apparatus (SCA20, DataPhysics Instruments). The advancing and receding contact angles (θ_A and θ_R) of the surfaces were measured at least in triplicate at an immersion speed of 0·12 μl s^{-1}.

Evaluation of rate of bacterial cell adhesion to membrane sheets. Bacterial adhesion tests were conducted in accordance with the method of Terada *et al.* (2005). The prepared cell suspension of 40 ml was placed in a 50 ml beaker. The concentrations of *E. coli* and *B. subtilis* cells were adjusted to provide an OD_{660} of 0·050; these concentrations were $5{\cdot}8 \times 10^9$ and $2{\cdot}3 \times 10^9$ cells ml^{-1}, respectively. PE, GMA, EA and DEA sheets were cut into 0·25 cm^2 sections. Each sheet was immersed in a beaker containing an *E. coli* or *B. subtilis* cell suspension. The cell suspension and the prepared sheets were agitated at 200 r.p.m. at 25 °C. The adhesion of the cells onto each sheet was estimated from the decrease in the OD_{660} of each cell suspension. The adhesion rate constant *k* was defined as follows (Lee *et al.*, 1996)

$$V \frac{dC}{dt} = -kAC \quad (4)$$

$$k = -\left(\frac{V}{A} \right) \left(\frac{1}{t} \right) \ln \left(\frac{C_t}{C_0} \right) \quad (5)$$

where *V*, *A*, *t*, C_t and C_0 are the volume of the cell suspension, two-dimensional sheet surface area, contact time, OD_{660} at time *t* and initial OD_{660}, respectively.

Viability of bacterial cells adhering to membrane sheets. The viability of *E. coli* adhering to each sheet was evaluated using a commercially available staining kit (Live/Dead *Ba*dight bacterial viability kit, Molecular Probes). The Live/Dead kit included the green fluorescent DNA-binding stain SYTO 9 and the red fluorescent DNA-binding stain propidium iodide (PI), enabling the determination of bacterial viability from the difference in membrane integrity in embedded cells (Boulos *et al.*, 1999). In the case of *B. subtilis*, a mixture of YO-PRO-1 and PI was applied instead of using the Live/Dead kit due to the difference in permeation of PI in Gram-positive and Gram-negative bacteria. We previously confirmed the suitability of the mixture by applying it to *B. subtilis* cells before and after immersion into 70 % ethanol solution for 15 min to detect inactive cells. Each membrane sheet was carefully removed from the beaker after immersion in a bacterial cell suspension and was mounted in a well on a glass slide. Each sheet was immersed in 8 μl 1000-fold-diluted Live/Dead kit solution or the mixture of YO-PRO-1 and PI and was incubated for 15 min in the dark. After washing with distilled water, the sheets were mounted in FluoroGuard Antifade reagent (Bio-Rad), and observed using a fluorescence microscope (Axioskop2 plus, Carl Zeiss) to visualize intact and damaged cells. Bacterial viability was calculated from the ratio of the number of intact cells stained with SYTO-9 or YO-PRO-1 to the total number of cells [intact plus PI-positive (damaged) cells]. Direct counts were made for at least 10 randomly recorded images.

RESULTS

Characterization of membrane sheets prepared by RIGP

The *dg* of the membrane sheets increased proportionally to reaction time in 5 % (w/w) GMA/methanol solution ($r^2 = 0{\cdot}996$; see Fig. S1, available with the online version of this paper). The time courses of the conversion of the grafted epoxy groups to amino groups are shown in Fig. 2. The molar conversion percentages of the epoxy groups relative to the amino groups ranged from 9 % to 98 %. Although the time for conversion differed between EA and DEA sheets, the results clearly indicate the possibility of controlling the conversion ratio of amino groups. Fig. 3 shows the relationship between the density of the EA and DEA groups determined by titration and that determined from weight gain calculated using equation (2). A good agreement was found, which indicates that the weight gain accompanying the reaction of the epoxy group with EA or DEA corresponded to the intrinsic introduction of these groups. This result clearly suggests that the increase in weight was due

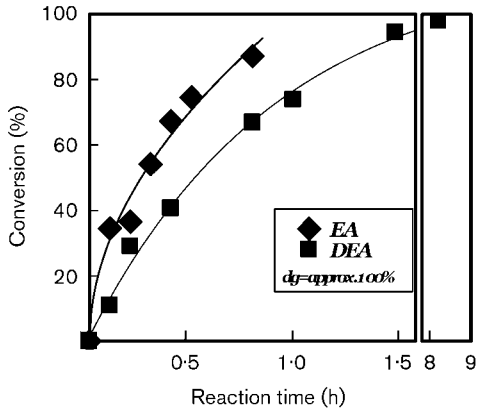

Fig. 2. Time courses of conversion of epoxy groups to EA and DEA groups.

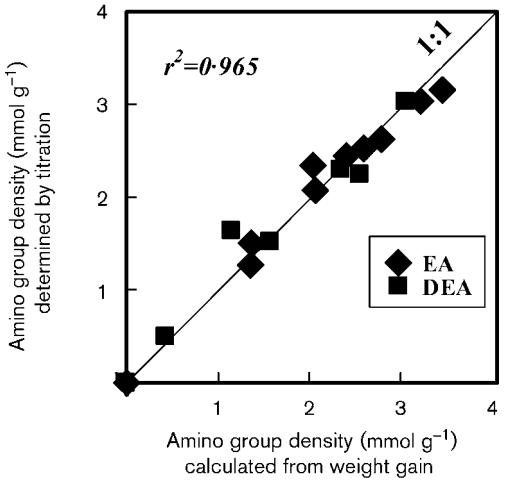

Fig. 3. Amino group densities determined by titration vs those calculated from weight gain.

to the conversion of GMA to EA or DEA, supporting the accuracy of the conversion reaction in this experiment. The relationship between amino group density and membrane potential is shown in Fig. 4. This figure clearly shows that the

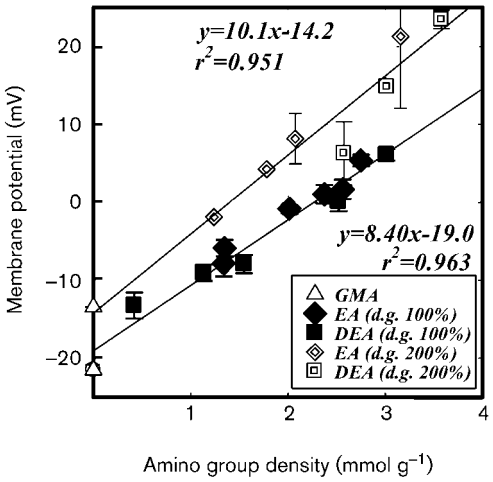

Fig. 4. Relationship of amino group density and membrane potential.

membrane potentials of the EA and DEA sheets were proportional to their amino group densities irrespective of *dg*, although the degree of each slope, which shows the relationship between amino-group density and membrane potential, is different. The results of water contact angle are summarized in Table 1. Equilibrium water contact angles were marginally affected by the grafted surfaces, regardless of the introduction of amino groups, although the advancing contact angle of the grafted surfaces slightly increased, whereas the receding contact angle decreased. Furthermore, an increase in amino group density (or membrane potential) caused a decrease in receding contact angle (an increase of contact angle hysteresis), demonstrating that contact angle hysteresis was proportional to membrane potential (see Fig. S2, available with the online version of this paper) for *dg* values of both 100 % and 200 %. Such a relationship is probably due to the amino groups being hydrophilic, which is generated through conversion of GMA to EA or DEA.

Estimation of bacterial cell adhesion

It was confirmed that the reduction of bacterial cell concentration proceeded in the manner of a first-order reduction and that errors in the bacterial cell adhesion

Table 1. Contact angles of PE, GMA, EA and DEA sheets

EA 1 and 2 and DEA 1 and 2 are sheets with different amino group densities. Standard deviations are given in parentheses ($n=3$).

	PE	GMA	EA 1	EA 2	DEA 1	DEA 2
Degree of grafting (%)	–	100	100	100	100	100
Amino group density (mmol g^{-1})	–	–	0·26	2·91	0·28	2·88
Equilibrium contact angle (°)	96·7 (±3·2)	98·7 (±6·7)	97·0 (±4·8)	96·1 (±3·4)	95·5 (±3·6)	96·0 (±2·8)
Advancing contact angle (°)	96·5 (±2·2)	107·1 (±3·1)	105·4 (±2·6)	107·7 (±4·3)	104·5 (±0·84)	106·6 (±4·9)
Receding contact angle (°)	70·5 (±1·7)	77·1 (±5·0)	57·1 (±3·9)	47·9 (±6·7)	60·5 (±0·5)	46·1 (±4·5)
Contact angle hysteresis (°)	26·0	30·0	48·3	59·8	44·0	60·5

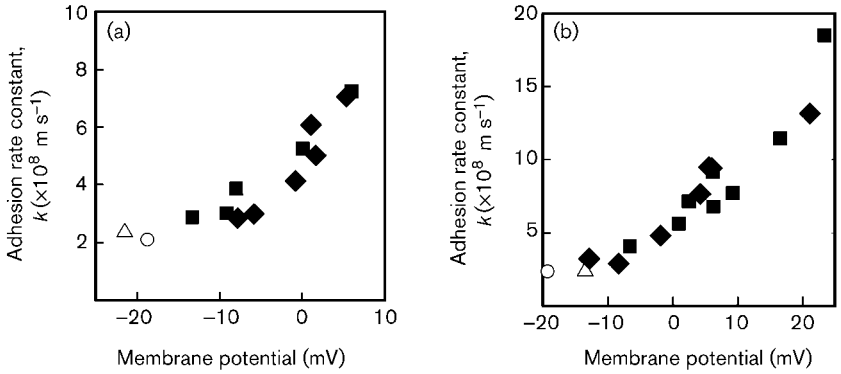

Fig. 5. Effect of membrane potential on adhesion rate constant k for *E. coli* (a) and *B. subtilis* (b). ○, PE; △, GMA; ◆, EA; ■, DEA.

experiment were less than 10 %, thereby ensuring the accuracy of this method (data not shown). Additional experiments confirmed that the concentration change derived from cell growth and adhesion to a beaker surface was less significant than that by bacterial adhesion to a sheet surface (see Fig. S3, available with the online version of this paper). The relationship between membrane potential and bacterial adhesion rate constant k is summarized in Fig. 5. For the PE and GMA sheets, the concentration of the bacterial cell suspensions did not decrease significantly (less than 10 % decrease relative to the initial bacterial concentration), leading to a low adhesion rate constant k. The rate constants for the EA and DEA sheets increased with their membrane potentials. It should be noted that the rate constant slightly increased with an increase in the sheet membrane potential up to −7·8 mV and −8·3 mV in cases of *E. coli* and *B. subtilis* cell adhesion (*E. coli*: linear correlation, $y=0{\cdot}056x+3{\cdot}41$, $r^2=0{\cdot}733$; *B. subtilis*: linear correlation, $y=0{\cdot}110x+4{\cdot}31$, $r^2=0{\cdot}611$), whereas it significantly increased at more than these membrane potentials (*E. coli*: linear correlation, $y=0{\cdot}332x+5{\cdot}08$, $r^2=0{\cdot}926$; *B. subtilis*: linear correlation, $y=0{\cdot}408x+5{\cdot}99$, $r^2=0{\cdot}884$). Such a two-gradient increase in the rate constant might be related to the electrostatic and hydrophobic interactions, both of which will be discussed below.

Evaluation of bacterial viability

The time courses of the transition of bacterial viability on the PE, GMA, EA and DEA sheets are shown in Fig. 6. The viability of both *E. coli* and *B. subtilis* cells in the planktonic state remained approximately 90 % after 8 h and 6 h in the bulk liquid in which each sheet was immersed. There was no dissolution of amino groups from any of the polymer sheets, and the effect of the bulk liquid on the viability of bacterial cells was negligible; both results were confirmed by measuring the density of each sheet before and after the blank experiment devoid of bacterial cells (see Fig. S4, available with the online version of this paper). Similar tendencies between the PE and GMA sheets were observed: 70–80 % of adhering *E. coli* cells on the PE and GMA sheets were viable, and the viability remained almost constant during the entire experimental period, although viability slightly decreased over time (Fig. 6a). Although the growth or decay of *E. coli* on these sheets might affect viability, preliminary experiments showed no significant change in viability (data not shown). On the other hand, the trends of *E. coli* viability on the EA (87) and DEA (95) sheets were quite different from those on the PE and GMA sheets. The *E. coli* viabilities of the EA (87) and DEA (95) sheets were quite low even at 0·25 h. After immersion of these three sheets in the *E. coli* cell suspension for 8 h, the percentage viability decreased to 20–30 % irrespective of the differences among secondary and tertiary amino groups, indicating that large numbers of *E. coli* cells were inactive after adhesion to the EA (87) and DEA (95) sheets. In the case of *B. subtilis*, the same trend was observed for the PE and GMA sheets: approximately 80 % of *B. subtilis* cells on the sheets remained viable. An intriguing observation is that the viability of *B. subtilis* on

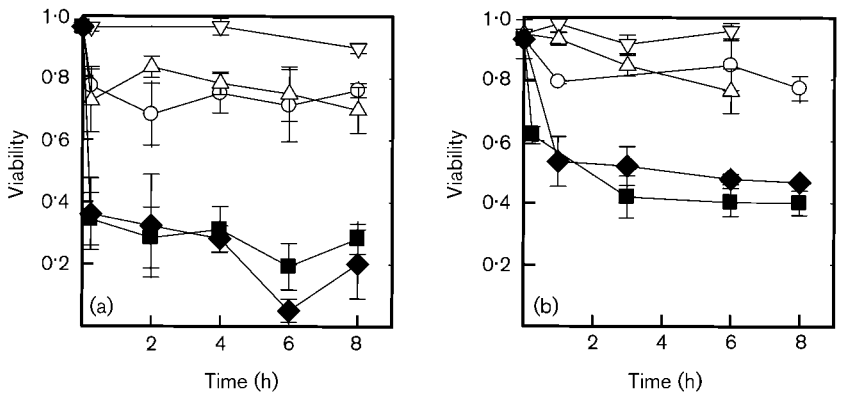

Fig. 6. Time-courses of *E. coli* (a) and *B. subtilis* (b) viability on PE, GMA, EA and DEA sheets. (a) ▽, Planktonic; ○, PE; △, GMA; ◆, EA (87); ■, DEA (95). (b) ▽, Planktonic; ○, PE; △, GMA; ◆, EA (83); ■, DEA (72).

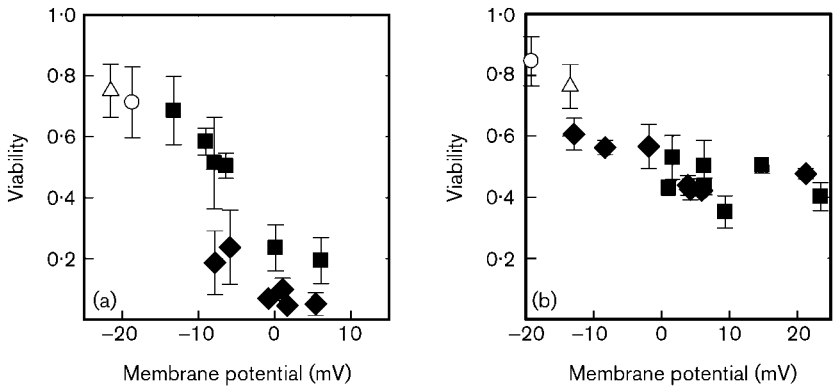

Fig. 7. Dependence on sheet membrane potential of the viability of *E. coli* (a) and *B. subtilis* (b) after 6 h. ○, PE; △, GMA; ◆, EA; ■, DEA.

the EA (83) and DEA (72) sheets did not rapidly decrease during the first 1 h of immersion of the cell suspension, in contrast to *E. coli* cells (Fig. 6b). Furthermore, the viability of *B. subtilis* on the EA (83) and DEA (72) sheets ranged from 0·4 to 0·45 even after 8 h immersion in the cell suspension, rates higher than those of *E. coli* cells.

The relationship between membrane potential and viability after 6 h immersion in the cell suspension is shown in Fig. 7. In both bacterial strains, viability on the EA and DEA sheets was dependent on the membrane potentials of the sheets. A critical point of *E. coli* viability was clearly observed (Fig. 7a); the viability decreased significantly at membrane potentials higher than −8 mV. At other sampling times (0·25, 2, 4 and 8 h), sharp decreases in *E. coli* viability were also observed at almost the same point (see Fig. S5, available with the online version of this paper), indicating that the membrane potentials of these sheets strongly affected *E. coli* viability. Although the exact reason for this decrease in activity remains unclear, we have demonstrated that amino-group-containing sheets, i.e. the EA and DEA sheets, with a membrane potential higher than −8 mV significantly inactivated *E. coli* cells and that there was a membrane potential threshold for the decrease in the activity of *E. coli* cells. In contrast, such a membrane potential threshold was not observed for *B. subtilis*. The viability slightly decreased from 0·8 to approximately 0·4 with an increase in membrane potential. Such different trends may possibly stem from different cell wall structures in these two bacterial species. This is discussed further in the Discussion.

DISCUSSION

Predominant effects on bacterial adhesion

The relationship between the surface roughness of membrane sheets and the *dg* has previously been investigated, leading to the conclusion that the roughness increases linearly with *dg* irrespective of functional group, i.e. DEA and GMA (Terada *et al.*, 2005). Although sheets with *dg* values of approximately 100 % and 200 % were used in this study, the effect of roughness (except for the PE membrane) was less significant than that of amino-group density; hence, the effect of roughness on bacterial cell adhesion should be marginal. Dynamic contact angle measurement indicated that positively charged surfaces, derived from the introduction of ethylamine and diethylamine to the GMA sheet, increased the degree of hydrophilicity (Table 1), resulting in a large contact angle hysteresis. Furthermore, membrane potential, proportional to amino group density (Fig. 4), was correlated with contact angle hysteresis [linear correlation: $y=0{\cdot}936x-51{\cdot}6$ ($r^2=0{\cdot}972$) and $y=0{\cdot}716x-26{\cdot}0$ ($r^2=0{\cdot}819$) at *dg* values of 100 % and 200 %, respectively; see Fig. S2]. In light of this correlation, two factors, i.e. hydrophobic/hydrophilic interactions and electrostatic interactions, would appear to be predominantly involved in bacterial adhesion, as previously reported (Li & Logan *et al.*, 2004; van Loosdrecht *et al.*, 1990; Webb *et al.*, 1998). It is well known that bacterial cells have predominantly negative charges on their surfaces, irrespective of whether they are Gram-positive or Gram-negative; hence, electrostatic interaction increases with increasing membrane potential, as shown in Fig. 5. In addition, bacterial hydrophobicity is dependent on cell wall structure. Generally, Gram-negative bacteria such as *E. coli* contain LPS in their cell envelope, which attracts a water layer resulting in a high degree of hydrophilicity; in contrast, Gram-positive bacteria such as *B. subtilis* do not contain LPS, resulting in a high degree of hydrophobicity (Li & Logan, 2004). In light of the assumption that surfaces with high membrane potential should be more hydrophilic because of high concentrations of amino groups, hydrophilic interaction between *B. subtilis* and the surface works against their adhesion, resulting in a decrease in the adhesion rate constant. Nevertheless, the result of the adhesion experiments on *B. subtilis* cells indicated that surfaces with high membrane potential have characteristics which enhanced adhesion of *B. subtilis* cells (Fig. 5b). Such an understanding supports the argument that the effect of membrane potential on enhancement of *B. subtilis* cell adhesion prevails against that of hydrophilic interaction, leading to the conclusion that electrostatic interaction, i.e. membrane potential, would be the most significant parameter in *B. subtilis* cell adhesion. Meanwhile, the predominant effect on *E. coli* cells could not be determined specifically since the degree of hydrophilicity, likely to enhance *E. coli* cell adhesion, was proportional to that of membrane potential. Reportedly, the contribution of both membrane potential and contact angle hysteresis to

bacterial adhesion is dependent on the presence of proteins commonly excreted during cell growth (Webb *et al.*, 1998). Webb *et al.* (1998) reported that the presence of positively charged functional groups is the primary factor promoting increased cell adhesion in the absence of these proteins. Since organic carbon was not supplied during the adhesion experiments, excretion of protein would be expected to have been low, supporting the possibility that dominant effects could be electrostatic interactions, although the contribution of thermodynamics, i.e. hydrophobic interaction, cannot be ignored.

Effect of graft chain on bacterial cell adhesion

The determination of the behaviour of *E. coli* and *B. subtilis* adhesion on the prepared sheets shows that the adhesion rate constants increased with membrane potential and that the increases became steep at membrane potentials greater than −7·8 mV and −8·3 mV, respectively (Fig. 5). Such a sharp increase in adhesion rate constant implies that interactions other than electrostatic effects and surface wettability are involved in enhancement of cell adhesion. The sheets prepared by RIGP have a very unusual structure, i.e. they have graft chains containing amino groups with a positive charge, and this attracts bacterial cells (Kawai *et al.*, 2003). Therefore, this would seem to be important in elucidating how these polymer conformations influence bacterial adhesion. Tsuneda *et al.* (1992) showed that a threshold to decrease water flux through a hollow-fibre membrane with DEA-containing graft chains was observed above a 40–60 % DEA conversion, which indirectly suggests extension of the grafted chains. It has been reported that the DEA-containing graft chains extend with the capture of proteins due to electrostatic repulsion between each DEA group in water, and that ionizable graft chains can form distinct conformational structures, depending on the density of ionizable groups (Kawai *et al.*, 2000; Koguma *et al.*, 2000). These two reports indirectly inferred an extension of the graft chains, resulting in drastic changes in water permeability and protein attachment. In our study, the sheet with 40–60 % DEA conversion had a membrane potential of approximately −8 mV, coinciding with the point at which the gradient of adhesion rate constant with membrane potential and the viability threshold for *E. coli* were observed. Hitherto, there have been no reports of microscopic proof that such extension of polymer chains occurs; hence, we cannot conclude that there is definitely involvement of graft chain extension. Nevertheless, such a supposition would suggest that the enhancement of bacterial adhesion is due to favourable membrane potential and hydrophobicity of surfaces for *E. coli* and *B. subtilis* cells, and possibly to the extension of graft chains induced by electrostatic repulsion among graft chains.

Are RIGP-treated sheets effective in biofilm inhibition and promotion?

The results in Fig. 7 show that the viability of *E. coli* and *B. subtilis* cells was dependent on membrane potential irrespective of the differences between secondary and tertiary amino groups. Apparently, there was a threshold, around a membrane potential of −8 mV, which governed the viability of *E. coli* cells. Therefore, the membrane potential of the sheets could be a crucial factor affecting not only bacterial adhesion rate but also bacterial viability. On the other hand, a threshold was not observed in the case of *B. subtilis*. Moreover, the viability of *B. subtilis* cells remained higher than that of *E. coli* cells. Such differences in behaviour are presumably due to differences in external cell structure in Gram-positive and Gram-negative bacteria. Two mechanisms for the loss of bacterial activity on polymer chains with anion-exchange groups, e.g. quaternary ammonium compounds, have been suggested (Kügler *et al.*, 2005; McDonnell & Russell, 1999; Salton, 1968; Tiller *et al.*, 2001). One of these mechanisms would be expected to operate in Gram-negative bacteria (Vaara, 1992): polymer chains with positively charged surfaces displace divalent cations (e.g. Ca^{2+} and Mg^{2+}), which hold together the negatively charged surface of the lipopolysaccharide network, thereby disrupting the outer membrane of Gram-negative bacteria such as *E. coli*. The other mechanism is likely to operate when the positively charged polymer chains penetrate into the inner membrane, leading to cell leakage and eventually inactivation (Lin *et al.*, 2003). In the case of *E. coli* (Fig. 7a), either mechanism would be sufficient to be lethal. In addition, there should be a possibility of involvement of graft chain extension in the inactivation of *E. coli* cells as described above. Furthermore, since Gram-positive bacteria, e.g. *B. subtilis*, have a thicker external layer of peptidoglycan compared to Gram-negative bacteria (Li & Logan, 2004), the antibacterial effect of the length of the grafted chains is not sufficient in *B. subtilis*, resulting in maintenance of viability (approx. 0·4) in spite of the surface having a high membrane potential. Therefore, it should be noted that sufficient lengths of grafted polymer chain with amino groups would be required to reach the cytoplasmic membrane of *B. subtilis* and eventually to inactivate cells. On the other hand, lengths which do not reach the cytoplasmic membrane would be expected to be advantageous in biofilm promotion. Since RIGP can provide control of the grafted length by adjustment of reaction time in a monomer solution such as GMA, optimum designs for sheets for biofilm inhibition or promotion may be possible. Although such designs should be addressed in future studies, the viability results in this study clearly demonstrate that surfaces with high membrane potentials affect the viability of bacteria adhering to polymer surfaces.

Some researchers have focused on the effects of positively charged surface properties on biofilm formation. Gottenbos *et al.* (2001) showed that bacterial adhesion to a surface with positive zeta potential is enhanced; however, subsequent biofilm formation is slower, indicating that a positively charged surface adversely affects biofilm formation. On the other hand, Hibiya *et al.* (2000) reported that a nitrifying biofilm, which is difficult to obtain, forms on DEA-containing sheets successfully under high hydrodynamic

conditions. This apparent conflict may be due to the fact that different surface properties, bacterial concentrations and hydrodynamic conditions were used in these studies, and hence it is difficult to systematically summarize the crucial factors in biofilm formation. Moreover, Lee *et al.* (2004) observed, by atomic force microscopy, that EPS from dead *E. coli* cells adsorbed onto glass surfaces, although it is unclear how EPS works after cell death. Tsuneda *et al.* (2001) reported that the utilization of EPS excreted by heterotrophic bacteria results in a thick biofilm with large numbers of the autotrophic nitrite-oxidizing bacterium *Nitrobacter winogradskyi*, and a high nitrite-oxidation rate. Since the EPS excreted by dead *E. coli* cells could help the biofilm adhere strongly and supply carbon components to live cells, sheets with high membrane potential seem to have an advantage in biofilm formation under turbulent flow conditions. Our ongoing research is focused on the long-term activity of bacterial cells adhering to PE, GMA, EA and DEA sheets and on subsequent biofilm formation in a flow chamber, which will elucidate the differences between the mechanisms of the formation of a series of biofilms dependent on surface properties. The adhesion assay used in this study is not applicable to monitoring subsequent biofilm formation because bacteria from the bulk liquid inevitably attach to the biofilm, leading to erroneous estimates. Biofilm formation experiments using a flow chamber, which have been conducted by many researchers, can probably overcome this problem and facilitate *in situ* observation of grown biofilms (Bos *et al.*, 1999; Busscher & van der Mei, 1995; Stoodley & Warwood, 2003), leading to strategies for optimum biointerface designs for the inhibition or promotion of biofilm formation.

Conclusions

A monomer containing an epoxy group, GMA, was grafted onto a PE sheet. Two amino groups, EA and DEA, were added to the grafted sheets at different amino group densities. The anion-exchange capacities determined both membrane potential and surface hydrophobicity. Membrane potential is likely to be a good indicator of the rate of bacterial adhesion to the EA and DEA sheets since the adhesion rate constant increases with membrane potential. The viability of *E. coli* and *B. subtilis* cells on the positively charged EA and DEA sheets with high membrane potential decreased with increasing membrane surface potential in comparison with these bacteria on the PE and GMA sheets. Furthermore, a membrane potential threshold critically affecting the viability of *E. coli*, but not that of *B. subtilis*, was observed, suggesting that differences in their cell wall structures are likely to affect viability. Since EA and DEA sheets have high bacterial adhesion properties, they do not seem to be suitable for bacterial biofilm inhibition. Although we do not yet know whether these sheets can be used to promote biofilm formation, the results obtained in this study at least suggest that differences in surface properties influence adhesion behaviour and the viability of adhering bacteria, both of which are closely related to biofilm formation.

ACKNOWLEDGEMENTS

We are grateful to Dr Wako Takami of Asahi Kasei Chemicals Corporation for providing the membrane sheets, to Dr Hiroshi Hayashi of Mitsubishi Material Corporation for helpful advice on bacterial adhesion, and to Professor Shuji Ohwada and Ms Yoshiko Yamamoto for measurements of dynamic contact angle. One of the authors, A. Terada, was supported by a Research Fellowship for Young Scientists from the Japan Society for the Promotion of Science (JSPS) during this study.

REFERENCES

Bos, R., van der Mei, H. C. & Busscher, H. J. (1999). Physico-chemistry of initial microbial adhesive interactions – its mechanisms and methods for study. *FEMS Microbiol Rev* **23**, 179–230.

Boulos, L., Prevost, M., Barbeau, B., Coallier, J. & Desjardins, R. (1999). LIVE/DEAD® *Bac*Light™: application of a new rapid staining method for direct enumeration of viable and total bacteria in drinking water. *J Microbiol Methods* **37**, 77–86.

Busscher, H. J. & van der Mei, H. C. (1995). Use of flow chamber devices and image analysis methods to study microbial adhesion. In *Adhesion of Microbial Pathogens Methods in Enzymology*, pp. 455–477. Edited by R. J. Doyle & I. Ofek. San Diego: Academic Press.

Busscher, H. J., Bos, R. & van der Mei, H. C. (1995). Initial microbial adhesion is a determinant for the strength of biofilm adhesion. *FEMS Microbiol Lett* **128**, 229–234.

Fox, P., Suidan, M. T. & Bandy, J. T. (1990). A comparison of media types in acetate fed expanded-bed anaerobic reactors. *Water Res* **24**, 827–835.

Gottenbos, B., van der Mei, H. C., Busscher, H. J., Grijpma, D. W. & Feijnen, J. (1999). Initial adhesion and surface growth of *Pseudomonas aeruginosa* on negatively and positively charged poly(methacrylates). *J Mater Sci Mater Med* **10**, 853–855.

Gottenbos, B., van der Mei, H. C. & Busscher, H. J. (2000). Initial adhesion and surface growth of *Staphylococcus epidermidis* and *Pseudomonas aeruginosa* on biomedical polymers. *J Biomed Mater Res* **50**, 208–214.

Gottenbos, B., Grijpma, D. W., van der Mei, H. C., Feijnen, J. & Busscher, H. J. (2001). Antimicrobial effects of positively charged surface on adhering Gram-positive and Gram-negative bacteria. *J Antimicrob Chemother* **48**, 7–13.

Hallam, N. B., West, J. R., Forster, C. F. & Simms, J. (2001). The potential for biofilm growth in water distribution systems. *Water Res* **35**, 4063–4071.

Harris, L. G. & Richards, R. G. (2004). *Staphylococcus aureus* adhesion to different treated titanium surfaces. *J Mater Sci Mater Med* **15**, 311–314.

Hendricks, S. K., Kwok, C., Shen, M. C., Horbett, T. A., Ratner, B. D. & Bryers, J. D. (2000). Plasma-deposited membranes for controlled release of antibiotic to prevent bacterial adhesion and biofilm formation. *J Biomed Mater Res* **50**, 160–170.

Hibiya, K., Tsuneda, S. & Hirata, A. (2000). Formation and characteristics of nitrifying biofilm on a membrane modified with positively-charged polymer chains. *Colloids Surf B Biointerfaces* **18**, 105–112.

Kawai, T., Sugita, K., Saito, K. & Sugo, T. (2000). Extension and shrinkage of polymer brush grafted onto porous membrane induced by protein binding. *Macromolecules* **33**, 1306–1309.

Kawai, T., Saito, K. & Lee, W. (2003). Protein binding to polymer brush, based on ion-exchange, hydrophobic, and affinity interactions. *J Chromatogr B* **790**, 131–142.

Kjellerup, B. V., Olesen, B. H., Nielsen, J. L., Frolund, B., Odum, S. & Nielsen, P. H. (2003). Monitoring and characterisation of bacteria in corroding district heating systems using fluorescence in situ hybridisation and microautoradiography. *Water Sci Technol* **47**, 117–122.

Koguma, I., Sugita, K., Saito, K. & Sugo, T. (2000). Multilayer binding of proteins to polymer chains grafted onto porous hollow-fiber membranes containing different anion-exchange groups. *Biotechnol Prog* **16**, 456–461.

Kügler, R., Bouloussa, O. & Rondelez, F. (2005). Evidence of a charge-density threshold for optimum efficiency of biocidal cationic surfaces. *Microbiology* **151**, 1341–1348.

Lee, W., Furusaki, S., Saito, K., Sugo, T. & Makuuchi, K. (1996). Adsorption kinetics of microbial cells onto a novel brush-type polymeric material prepared by radiation-induced graft polymerization. *Biotechnol Prog* **12**, 178–183.

Lee, W., Saito, K., Furusaki, S. & Sugo, T. (1997). Capture of microbial cells on brush-type polymeric materials bearing different functional groups. *Biotechnol Bioeng* **53**, 523–528.

Lee, W., Saito, K., Furusaki, S. & Sugo, T. (1998). Tailoring a brush-type interface favorable for capturing microbial cells. *J Colloid Interface Sci* **200**, 66–73.

Lee, S. B., Koepsel, R. R., Morley, S. W., Matyjaszewski, K., Sun, Y. & Russell, A. J. (2004). Permanent, nonleaching antibacterial surfaces. 1. Synthesis by atom transfer radical polymerization. *Biomacromolecules* **5**, 877–882.

Li, B. K. & Logan, B. E. (2004). Bacterial adhesion to glass and metal-oxide surfaces. *Colloids Surf B Biointerface* **36**, 81–90.

Lin, J., Qiu, S. Y., Lewis, K. & Klibanov, A. M. (2003). Mechanism of bactericidal and fungicidal activities of textiles covalently modified with alkylated polyethylenimine. *Biotechnol Bioeng* **83**, 168–172.

Lin, W., Yu, T., McSwain, B. S. & He, Y. L. S. (2004). Biological fixed film systems. *Water Environ Res* **76**, 1099–1154.

McDonnell, G. & Russell, A. D. (1999). Antiseptics and disinfectants: activity, action, and resistance. *Clin Microbiol Rev* **12**, 147–179.

Morgan, T. D. & Wilson, M. (2001). The effects of surface roughness and type of denture acrylic on biofilm formation by *Streptococcus oralis* in a constant depth film fermentor. *J Appl Microbiol* **91**, 47–53.

Nicolella, C., van Loosdrecht, M. C. M. & Heijnen, J. J. (2000). Wastewater treatment with particulate biofilm reactors. *J Biotechnol* **80**, 1–33.

Park, K. D., Kim, Y. S., Han, D. K., Kim, Y. H., Lee, E. H. B., Suh, H. & Choi, K. S. (1998). Bacterial adhesion on PEG modified polyurethane surfaces. *Biomaterials* **19**, 851–859.

Pasmore, M., Todd, P., Smith, S., Baker, D., Silverstein, J., Coons, D. & Bowman, C. N. (2001). Effects of ultrafiltration membrane surface properties on *Pseudomonas aeruginosa* biofilm initiation for the purpose of reducing biofouling. *J Membr Sci* **194**, 15–32.

Petrozzi, S., Kut, O. M. & Dunn, I. J. (1993). Protection of biofilms against toxic shocks by the adsorption and desorption capacity of carriers in anaerobic fluidized bed reactors. *Bioprocess Eng* **9**, 47–59.

Roosjen, A., Kaper, H. J., van der Mei, H. C., Norde, W. & Busscher, H. J. (2003). Inhibition of adhesion of yeasts and bacteria by poly(ethylene oxide)-brushes on glass in a parallel plate flow chamber. *Microbiology* **149**, 3239–3246.

Roosjen, A., van der Mei, H. C., Busscher, H. J. & Norde, W. (2004). Microbial adhesion to poly (ethylene oxide) brushes: influence of polymer chain length and temperature. *Langmuir* **20**, 10949–10955.

Salton, M. R. J. (1968). Lytic agents, cell permeability and monolayer penetrability. *J Gen Physiol* **52**, 252–277.

Stoodley, P. & Warwood, B. K. (2003). Use of flow cells and annular reactors to study biofilms. In *Biofilms in Medicine, Industry and Environmental Biotechnology*, pp. 197–213. Edited by P. Lens, A. P. Moran, T. Mahony, P. Stoodley & V. O'Flaherty. London: IWA Publishing.

Terada, A., Yamamoto, T., Hibiya, K., Tsuneda, S. & Hirata, A. (2004). Enhancement of biofilm formation onto surface-modified hollow-fiber membranes and its application to a membrane-aerated biofilm reactor. *Water Sci Technol* **49**, 263–268.

Terada, A., Yuasa, S., Tsuneda, S., Hirata, A., Katakai, M. & Tamada, M. (2005). Elucidation of dominant effect on initial bacterial adhesion onto polymer surfaces prepared by radiation-induced graft polymerization. *Colloids Surf B Biointerfaces* **43**, 99–107.

Tiller, J. C., Liao, C. J., Lewis, K. & Klibanov, A. M. (2001). Designing surfaces that kill bacteria on contact. *Proc Natl Acad Sci* **98**, 5981–5985.

Tsuneda, S., Saito, K., Furusaki, S., Sugo, T. & Ishigaki, I. (1992). Water/acetone permeability of porous hollow-fiber membrane containing diethylamino groups on the grafted polymer branches. *J Membr Sci* **71**, 1–12.

Tsuneda, S., Park, S., Hayashi, H., Jung, J. & Hirata, A. (2001). Enhancement of nitrifying biofilm formation using selected EPS produced by heterotrophic bacteria. *Water Sci Technol* **43**, 197–204.

Tsuru, T., Nakao, S. & Kimura, S. (1990). Effective charge-density and pore structure of charged ultrafiltration membranes. *J Chem Eng Jpn* **23**, 604–610.

Vaara, M. (1992). Agents that increase the permeability of the outer membrane. *Microbiol Rev* **56**, 395–411.

van Loosdrecht, M. C. M., Norder, W., Lyklema, J. & Zehnder, A. J. B. (1990). Hydrophobic and electrostatic parameters in bacterial adhesion. *Aquat Sci* **51**, 103–114.

Wang, Y., Kim, J. H., Choo, K. H., Lee, Y. S. & Lee, C. H. (2000). Hydrophilic modification of polypropylene microfiltration membranes by ozone-induced graft polymerization. *J Membr Sci* **169**, 269–276.

Webb, K., Hlady, V. & Tresco, P. A. (1998). Relative importance of surface wettability and charged functional groups on NIH 3T3 fibroblast attachment, spreading, and cytoskeletal organization. *J Biomed Mater Res* **41**, 422–430.